Politeknik Dergisi
Cilt: 7 Sayı: 1 s. 13-21, 2004

Journal of Polytechnic
Vol: 7 No: 1 pp. 13-21, 2004

STUDY OF SIMULTANEOUSLY DEVELOPING FLOW AND TEMPERATURE FIELD IN RECTANGULAR DUCTS WITH CONSTANT WALL TEMPERATURE

Halit KARABULUT, H. Serdar YÜCESU
Gazi University, Technical Education Faculty, Automotive Department,
06500 Teknikoklullar, ANKARA

ABSTRACT

In this research, the heat transfer and flow friction characteristics of hydrodynamically and thermally developing flows at the entrance of rectangular ducts have been theoretically studied. In calculating components of velocity, parabolic momentum equations were used. Temperature field was also determined using parabolic form of energy equation. Besides, pressure distribution was calculated by means of a Poisson equation, which is obtained from combination of momentum and continuity equations. In numerical solution of finite difference equations, Newton-Raphson method was used. Numerical results were presented for channels with 1/3, 2/3 and 3/3 aspect ratio and range of Reynolds number $250 \leq Re \leq 2250$. Accuracy of the analysis was confirmed by comparing the fully developed Nusselt numbers obtained in this study with the literature.

Key words: Compact heat exchanger, Laminar flow in rectangular duct, Inlet flow, Finite difference method

DİKDÖRTGEN KESİTLİ KANALLARDA SABİT DUVAR SICAKLIĞINDA EŞZMANLI GELİŞEN AKIŞIN ISI TRANSFERİNİN İNCELENMESİ

ÖZET

Bu çalışmada dikdörtgen kanalların girişinde hidrodinamik ve termal yönden gelişmekte olan akışın akış ve ısı transferi karakteristikleri teorik olarak incelenmiştir. Hız bileşenlerinin hesaplanmasında parabolik momentum denklemleri kullanılmıştır. Sıcaklık dağılımın belirlenmesinde ise enerji denkleminin parabolik biçimi kullanılmıştır. Basınç dağılımı, süreklilik ve momentum denklemlerinden elde edilen Poission denklemi yardımı ile belirlenmiştir. Sonlu fark denklemlerinin sayısal çözümlemelerinde Newton-Raphson metodu kullanılmıştır. Sayısal sonuçlar Reynold sayısının $250 \leq R e \leq 2250$ aralığında 1/3, 2/3 ve 3/3 kenar oranları için verilmiştir. Analizin doğruluğu literatürden elde edilen tam gelişmiş akışın Nusselt sayıları ile kıyaslanarak sağlanmıştır.

Anahtar Kelimeler: Kompakt ısı değiştiricileri, Dikdörtgen kanallarda laminer akış, Giriş bölgesi akışı, Sonlu farklar metodu

INTRODUCTION

The external flow heat transfer and flow friction characteristics of compact heat exchangers may be estimated via entrance flow analysis. Compact heat exchangers are installed with different external flow channels such as rectangle, triangle, hexagon, oval, etc. In the entrance of such channels, there appear three-dimensional flow and temperature fields. Estimation of heat transfer and flow friction is more laborious than circular ducts or parallel plates, which are two-dimensional patterns. The rectangular channel is the simplest case of the three-dimensional entrance flow.

At solid boundaries of flow field, boundary conditions are apparently known. However, at the inlet and outlet, boundary conditions are not so apparent. Velocity distributions at the inlet and outlet are parabolic, but undefined. At the inlet, in order to use a more authentic velocity distribution, Nguyen and Maclaine-cross (1) expanded the solution domain to include the upstream region of virtual entrance of the parallel plate channel. At the exit, Nguyen and Maclaine-cross (1) used the fully developed velocity distribution by taking the channel length large enough. However, in most of studies, the velocity distribution is assumed to be uniform at the virtual entrance of the channel, Schlichting (2), Cheng et al. (3), Gupta (4) and Magno et al. (5). The uniform inlet velocity is also valid for rectangular ducts. When governing equations are parabolized in z coordinate, the outlet boundary conditions required for velocity components are avoided.

For the estimation of nodal values of pressure, several difference equations were devised manipulating continuity and momentum equations, Shyy (6). It is also possible to transform the continuity and momentum equations into a Poisson type differential equation to describe the pressure field. The boundary conditions of this equation impose some difficulties. In flow direction, two boundary conditions are required, and both of them may be chosen as initial conditions. One of them may be a uniform pressure distribution as the other one is the pressure gradient. In air cooled heat

exchangers, since the front end of the channel is open to air, assuming the pressure gradient as zero may be reasonable. For solid boundaries, as demonstrated by Vradis et al. (7), derivative boundary conditions may be obtained by using the momentum equations perpendicular to the relevant boundaries. These type boundary conditions are second order accurate. At any cross cut of a rectangular duct, a circumferentially uniform boundary condition may be used in terms of pressure. Its value is determined by means of trial and error using the overall continuity equation; $\iint_A W\,dy\,dx = C$.

At rectangular air channels, two of four sides are outer surfaces of two parallel hot fluid channels as the other two are plate fins interconnecting the hot fluid channels to each other. On the fin surfaces, the temperature is slightly variable. On the surface of hot fluid channels, the temperature is less variable than that of fins. Therefore, the constant wall temperature is a pertinent boundary condition for temperature field. At the real entrance of an airflow channel, the temperature is equal to the ambient temperature. At the exit, the boundary condition is not known. However, by parabolizing the energy equation, the exit boundary condition is avoided.

The parallel plates entrance flow problem was first handled by H.Schlichting in 1934. Since then a large number of theoretical and experimental studies have been presented. Before 1980, flow and temperature field equations were solved using integral techniques, Schlichting (2). After 1980, in most of studies numerical methods have been used. Nguyen and Maclaine-cross (1) presented a numerical study where the Navier-Stokes equations are transformed into the vorticity transport equation and solved on a domain including upstream region of virtual entrance as well. As the result of study; Nusselt number, incremental heat transfer number and thermal entrance length are presented, where Pr ranged from 0.2 to 10.0 and Re ranged from 40 to 2000. Magno et al. (5), investigated the heat transfer characteristics of hydrodynamically and thermally developing entrance flow of the non-Newtonian power-law fluids. In the study boundary layer equations are solved with the generalized integral transform techniques. As the result, dimensionless temperature profiles and axial distribution of local Nusselt number was illustrated in diagrams.

The entrance flow heat transfer of rectangular duct is currently investigated. The problem is treated under three specific cases, namely slug flow, hydrodynamically developed thermally developing flow and thermally-hydrodynamically developing flow. For slug flow, Spiga and Morini (8) obtained an analytical solution in terms of orthogonal functions. They presented some cross cut temperature profiles and axial temperature profiles were presented. The fully developed Nusselt number and entrance length were illustrated as the function of aspect ratio. The normalized form of local Nusselt number with respect to the fully developed Nusselt number were also given in tables. For the case of hydrodynamically developed-thermally developing flow Sayed-Ahmed (9) conducted an numerical study to examine the heat transfer characteristics of a Herschel-Bulkley fluid, which is non-Newtonian. Variation of Nusselt number was studied for constant wall temperature and constant heat flux and illustrated in diagrams as function of Graetz number. Effect of viscous dissipation on the Nusselt number was also examined and illustrated as function of Brinkman and Graetz number.

Since the Prandtl number of air is about 1, in air-cooled heat exchangers the velocity and temperature profiles develop simultaneously. In the present study, the flow friction and heat transfer characteristics of entrance flow in rectangular ducts are investigated for flow and temperature fields simultaneously developing

PHYSICAL SYSTEM AND MATHEMATICAL MODEL

The physical mechanism of hydrodynamically and thermally developing flow is illustrated in Figure 1. The flow enters the channel with a uniform velocity and temperature distribution. Therefore, at the entrance edge of the channel wall, velocity and thermal boundary layers have zero thickness. In the flow direction, the thickness of velocity and temperature boundary layers increases. The heat flux and flow friction are dependent on the thermal and velocity boundary layers. The predominant velocity component within the flow field is the one parallel to the channel axis. In air cooled heat exchangers, the variation of density due to the temperature change is insignificant. The pressure variation has also an

insignificant effect on density, and therefore, the air is assumed to be incompressible.

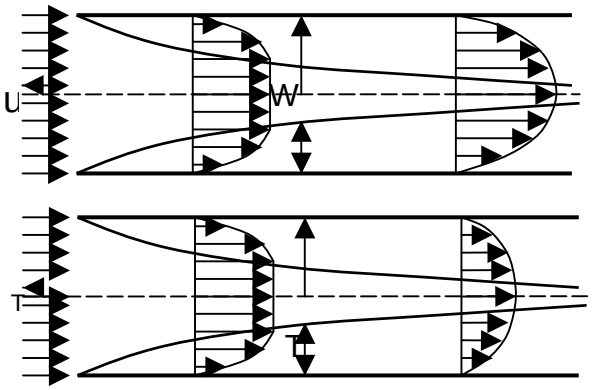

Figure 1. Velocity and Thermal Boundary Layers in Entrance Flow.

Coordinates are illustrated in Figure 2 where the flow direction is assumed to be the z coordinate.

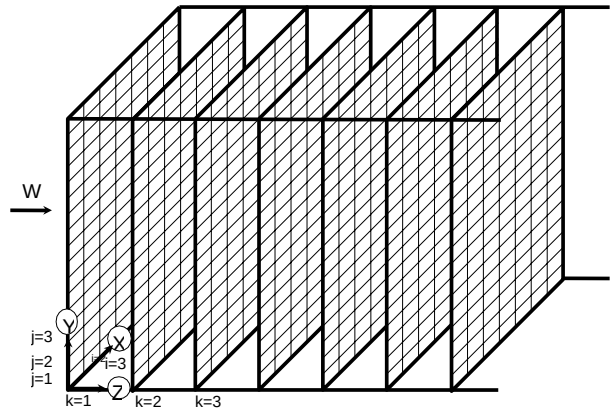

Figure 2. Coordinates and Grid Installation as the others are x and y. The non-dimensional forms of governing equations for flow field are,

$$U\frac{\partial U}{\partial X}+V\frac{\partial U}{\partial Y}+W\frac{\partial U}{\partial Z}= -\frac{1}{2}\frac{\partial \overline{P}}{\partial X}+\frac{1}{Re}\left[\frac{\partial^2 U}{\partial X^2}+\frac{\partial^2 U}{\partial Y^2}\right] \quad (1)$$

$$U\frac{\partial V}{\partial X}+V\frac{\partial V}{\partial Y}+W\frac{\partial V}{\partial Z}= -\frac{1}{2}\frac{\partial \overline{P}}{\partial Y}+\frac{1}{Re}\left[\frac{\partial^2 V}{\partial X^2}+\frac{\partial^2 V}{\partial Y^2}\right] \quad (2)$$

$$U\frac{\partial W}{\partial X}+V\frac{\partial W}{\partial Y}+W\frac{\partial W}{\partial Z}= -\frac{1}{2}\frac{\partial \overline{P}}{\partial Z}+\frac{1}{Re}\left[\frac{\partial^2 W}{\partial X^2}+\frac{\partial^2 W}{\partial Y^2}\right] \quad (3)$$

$$\frac{\partial}{\partial Z}\left(\iint_A W\,dY\,dX\right)=0 \quad (4)$$

$$\frac{\partial^2 \overline{P}}{\partial X^2}+\frac{\partial^2 \overline{P}}{\partial Y^2}+\frac{\partial^2 \overline{P}}{\partial Z^2}=\Phi \quad (5)$$

where,

$$Re=\frac{W_\infty D_h}{\nu},$$

$$\overline{P}=\frac{p}{\rho W_\infty^2/2},$$

$$\Phi=4\left(\frac{\partial U}{\partial X}\frac{\partial V}{\partial Y}-\frac{\partial U}{\partial Y}\frac{\partial V}{\partial X}+\frac{\partial U}{\partial X}\frac{\partial W}{\partial Z}-\frac{\partial U}{\partial Z}\frac{\partial W}{\partial X}+\frac{\partial V}{\partial Y}\frac{\partial W}{\partial Z}-\frac{\partial W}{\partial Y}\frac{\partial V}{\partial Z}\right).$$

For constant wall temperature, the governing equation of temperature field becomes,

$$U\frac{\partial \theta}{\partial X}+V\frac{\partial \theta}{\partial Y}+W\frac{\partial \theta}{\partial Z}= \frac{1}{Pr\,Re}\left[\frac{\partial^2 \theta}{\partial X^2}+\frac{\partial^2 \theta}{\partial Y^2}\right] \quad (6)$$

where,

$$\theta=(T-T_w)/(T_{in}-T_w).$$

Nusselt number is defined as,

$$Nu=\frac{1}{\theta_m}\left(\left|\frac{d\theta}{dn}\right|\right)_w. \quad (7)$$

The flow and temperature field equations are elliptic in x and y coordinates and parabolic in z coordinate. Boundary conditions are,

$$
\begin{array}{lllllll}
Z=0, & U=0, & V=0, & W=1, & \theta=1, & \bar{P}=\bar{P}_i, & \dfrac{\partial \bar{P}}{\partial Z}=0 \\
X=0, & U=0, & V=0, & W=0, & \theta=0, & \bar{P}=\bar{P}_w & \\
X=X_m, & U=0, & V=0, & W=0, & \theta=0, & \bar{P}=\bar{P}_w & \\
Y=0, & U=0, & V=0, & W=0, & \theta=0, & \bar{P}=\bar{P}_w & \\
Y=Y_m, & U=0, & V=0, & W=0, & \theta=0, & \bar{P}=\bar{P}_w &
\end{array}
$$

GRILLING OF SOLUTION DOMAIN AND FINITE DIFFERENCE EQUATIONS

Grilling of solution domain is illustrated in Figure 2 where i, j and k indicate number of grills in X, Y and Z coordinates respectively. In X and Y smaller, in Z larger grid sizes are used. In solving the finite difference equations, Newton-Raphson method is used. The U, V and W components of velocity are calculated from Equations 1, 2 and 3 respectively. In Newton-Raphson method, for the calculation of nodal values of U,

$$U^{n}_{i,j,k} = U^{n-1}_{i,j,k} - \frac{Ru}{\dfrac{\partial Ru}{\partial U^{n-1}_{i,j,k}}} \tag{8}$$

is used where U^{n-1} and U^{n} are estimated and corrected values of U, respectively, Burden and Douglas (10), Kincaid and Cheney (11). In entrance flow, the W component of velocity always takes positive values. The other components may take either positive or negative values. To obtain Ru from Equation 1, second order derivatives of U with respect to X and Y are replaced with their central difference approximations. The first order derivative of U with respect to Z is replaced with backward difference approximation. First order derivatives of U with respect to X and Y are replaced with their forward or backward difference approximations regarding whether U and V are positive or negative.

Using backward difference approximation for first order derivatives of U, Ru is stated as,

$$
\begin{aligned}
Ru = {} & \frac{U^{n-1}_{i,j,k}}{\Delta X}(U^{n-1}_{i,j,k} - U^{n-1}_{i-1,j,k}) + \\
& \frac{V^{n-1}_{i,j,k}}{\Delta Y}(U^{n-1}_{i,j,k} - U^{n-1}_{i,j-1,k}) + \\
& \frac{W^{n-1}_{i,j,k}}{\Delta Z}(U^{n-1}_{i,j,k} - U^{n-1}_{i,j,k-1}) \\
& - \frac{1}{Re\,\Delta X^2}(U^{n-1}_{i,j+1,k} - 2U^{n-1}_{i,i,k} + U^{n-1}_{i,j-1,k}) \\
& - \frac{1}{Re\,\Delta Y^2}(U^{n-1}_{i,j+1,k} - 2U^{n-1}_{i,j,k} + U^{n-1}_{i,j-1,k}) \\
& + \frac{1}{4\Delta X}(\bar{P}^{\,n-1}_{i-1,j,k} - \bar{P}^{\,n-1}_{i+1,j,k}).
\end{aligned} \tag{9}
$$

From the last equation,

$$
\begin{aligned}
\frac{\partial Ru}{\partial U^{n-1}_{i,j,k}} = {} & \frac{U^{n-1}_{i,j,k}}{\Delta X} + \frac{V^{n-1}_{i,j,k}}{\Delta Y} + \\
& \frac{W^{n-1}_{i,j,k}}{\Delta Z} + \frac{2}{Re\,\Delta X^2} + \frac{2}{Re\,\Delta Y^2}
\end{aligned} \tag{10}
$$

is obtained. If forward difference approximation of first order derivatives are used, Ru and $\dfrac{\partial Ru}{\partial U^{n-1}_{i,j,k}}$ become,

$$
\begin{aligned}
Ru = {} & \frac{U^{n-1}_{i,j,k}}{\Delta X}(U^{n-1}_{i+1,j,k} - U^{n-1}_{i,j,k}) + \\
& \frac{V^{n-1}_{i,j,k}}{\Delta Y}(U^{n-1}_{i,j+1,k} - U^{n-1}_{i,j,k}) + \\
& \frac{W^{n-1}_{i,j,k}}{\Delta Z}(U^{n-1}_{i,j,k} - U^{n-1}_{i,j,k-1}) \\
& - \frac{1}{Re\,\Delta X^2}(U^{n-1}_{i,j+1,k} - 2U^{n-1}_{i,i,k} + U^{n-1}_{i,j-1,k}) \\
& - \frac{1}{Re\,\Delta Y^2}(U^{n-1}_{i,j+1,k} - 2U^{n-1}_{i,j,k} + U^{n-1}_{i,j-1,k}) \\
& + \frac{1}{4\Delta X}(\bar{P}^{\,n-1}_{i-1,j,k} - \bar{P}^{\,n-1}_{i+1,j,k}).
\end{aligned} \tag{11}
$$

$$
\begin{aligned}
\frac{\partial Ru}{\partial U^{n-1}_{i,j,k}} = {} & -\frac{U^{n-1}_{i,j,k}}{\Delta X} - \frac{V^{n-1}_{i,j,k}}{\Delta Y} + \\
& \frac{W^{n-1}_{i,j,k}}{\Delta Z} + \frac{2}{Re\,\Delta X^2} + \frac{2}{Re\,\Delta Y^2}
\end{aligned} . \tag{12}
$$

If Ru is calculated using the same inputs in equation 9 and 11, almost the same results are obtained from both equations whatever the sign of U and V are. Therefore, in calculating Ru, any of above equations can be used. In calculating $\frac{\partial Ru}{\partial U_{i,j,k}^{n-1}}$ however, Equation 10 and 12 give different results. If U and V have positive values, Equation 10 is appropriate to use. In the case of U and V have negative values, all of the terms of Equation 12 will be positive and appropriate to use. If we state $\frac{\partial Ru}{\partial U_{i,j,k}^{n-1}}$ as

$$\frac{\partial Ru}{\partial U_{i,j,k}^{n-1}} = \left|\frac{U_{i,j,k}^{n-1}}{\Delta X}\right| + \left|\frac{V_{i,j,k}^{n-1}}{\Delta Y}\right| + \left|\frac{W_{i,j,k}^{n-1}}{\Delta Z}\right| + \frac{2}{Re\,\Delta X^2} + \frac{2}{Re\,\Delta Y^2} \quad (13)$$

Conditional use of 4 different equations will be avoided. Equation 13 is appropriate to use in all of the cases that U and V are positive, U and V are negative, U is positive and V is negative, or U is negative and V is positive. The other momentum equations and energy equation have the same feature and similarly discretized.

To solve Equation 5 by using Newton-Raphson method, nodal values of pressure is stated as,

$$\bar{P}_{i,j,k}^{\,n} = \bar{P}_{i,j,k}^{\,n-1} - \frac{Rp}{\frac{\partial Rp}{\partial \bar{P}_{i,j,k}^{\,n-1}}} \quad (14)$$

where,

$$Rp = \frac{1}{\Delta X^2}(\bar{P}_{i+1,j,k}^{\,n-1} - 2\bar{P}_{i,j,k}^{\,n-1} + \bar{P}_{i-1,j,k}^{\,n-1}) + \frac{1}{\Delta Y^2}(\bar{P}_{i,j+1,k}^{\,n-1} - 2\bar{P}_{i,j,k}^{\,n-1} + \bar{P}_{i,j-1,k}^{\,n-1}) + \frac{1}{\Delta Z^2}(\bar{P}_{i,j,k}^{\,n-1} - 2\bar{P}_{i,j,k-1}^{\,n-1} + \bar{P}_{i-1,j,k-2}^{\,n-1}) - \Phi_{i,j,k} \quad (15)$$

$$\frac{\partial Rp}{\partial \bar{P}_{i,j,k}^{\,n-1}} = -\frac{2}{\Delta X^2} - \frac{2}{\Delta Y^2} + \frac{1}{\Delta Z^2}. \quad (16)$$

Due to the nature of Newton-Raphson method, in the last equation ignoring the last term does not create any error in the result. Moreover, the other terms can also be multiplied by a convergence factor to speed up the iterative solution process.

In Z coordinate, since the problem is an initial value problem and two initial conditions are given for pressure field, solution is started from the third X-Y plain where $Z = 0$, and marched forward plain by plain as described by Madhav and Malin (12). The first and second grid plains are out of channel. At first, a reasonable pressure distribution is obtained by shooting a value for the wall boundary condition. In the first prediction of pressure distribution, nodal values of Φ are assumed to be zero all over the plain. After pressure distribution, the velocity components are predicted over the same plane, and nodal values of Φ are determined. Then, pressure distribution is iterated. By continuing to iterate the distribution of pressure and velocity components one after the other, the stable results are obtained, and then, the flow rate crossing the grid plain is determined. By correcting the flow rate by changing the wall boundary condition, the overall continuity is satisfied. Nodal values of pressure and velocity components obtained, correspondingly to the satisfaction of overall continuity, are the correct results. Then, over the subsequent plains, velocity components are similarly calculated.

Prediction of temperature field can be made after ending the flow field calculations all over the solution domain. It is also conducted plain by plain starting from the third plain. Since the boundary conditions of temperature field equation are apparently known, the calculation is straight forward.

RESULTS AND DISCUSSION

To ensure the consistency of the mathematical model with the theoretical expectations, velocity and temperature profiles are examined initially. In Figure 3, W profiles occurring on the X-Z midplain of the channel are illustrated. Numerical results used in Figure 3 are obtained for a channel having 1/3 aspect ratio and $Re = 375$. As expected, about the real entrance of the channel, W displays too big variation in the vicinity of the wall, and no variation about the center. As Z increases, profile of W converges to the fully developed velocity profile, which is seen on the same figure.

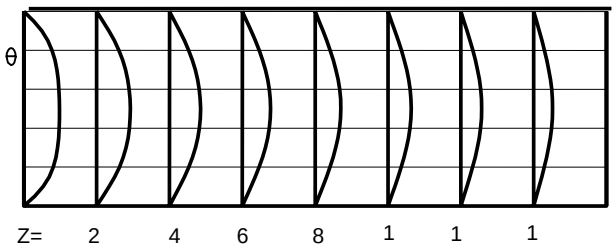

Figure 3. W Profiles in X-Z Midplain

Since the transition of entrance flow velocity profile to the fully developed velocity profile is an asymptotic variation, there is not a certain border between entrance flow and the fully developed flow region. In profiles of W, there appears a slight unsymmetry, which is plausibly due to the algorithm used in discretization.

If W profiles obtained in this analysis were compared to axial velocity profiles given by Schlichting (2) for parallel plates, important differences are seen. The axial velocity profiles represented by Schlichting are obtained from the solution of axial momentum and continuity equations, and the velocity profile, given for the virtual entrance of the channel is more likely the uniform velocity of the fluid entering the channel yet. The velocity profile obtained in this study for the virtual entrance of the channel is rather parabolic. Therefore, lower frictional losses and heat transfer coefficients are expected from this analysis.

In Figure 4, variation of V in Y coordinate is illustrated. The highest value of V which is $2.8 \cdot 10^{-2}$ appears on the grid plain at the real entrance of the channel. As Z increases, a sharp decrease in V is seen. Despite it is not illustrated in this study, U has similar profiles. Comparison of curves to each other indicates that a slight fluctuation exist.

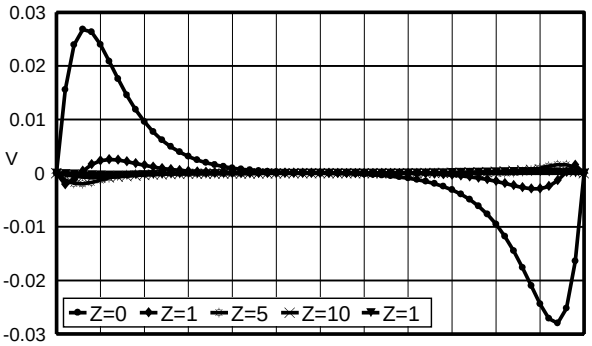

Figure 4. Variation of V Along Symmetry Axis of X-Y Plains

In the case of that fluid is hot and wall is cold, a dimensionless temperature profile in the form of D letter is expected. In Figure 5, dimensionless temperature profiles occurring in X-Z midplain are seen and consistent with expectations. The asymptote of dimensionless temperature profile is a vertical straight line. As seen in Figure 5, while Z increases, temperature profiles approach to a vertical straight line. In dimensionless temperature profiles also, a slight unsymmetry appears.

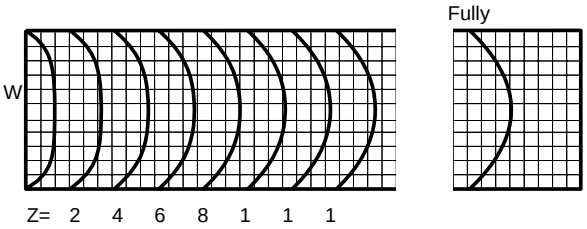

Figure 5. Temperature Profiles in X-Z Midplain

Figure 6, 7 and 8 illustrate the variation of the peripherally averaged local Nusselt number with axial distance for $1/3$, $2/3$ and $1/1$ aspect ratio. The horizontal straight line below the curves is the Nusselt number of the fully developed flow and temperature field. From down to up, curves correspond to 250, 375, 750, 1500 and 2250 values of Reynolds number, respectively. As expected the highest value of Nusselt number occurs at the real entrance of the duct. Since equations used for flow and temperature field are parabolic, local Nusselt number should be independent of aspect ratio but dependent on Reynolds number at the virtual entrance. As seen form Figure 6, 7, and 8, in great extend, expectation is confirmed. The small deviation may be due to the use of different values for dX and dY at different aspect ratios.

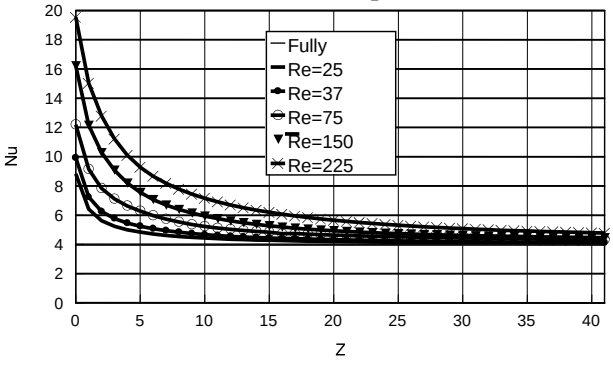

Figure 6. Variation of Nuselt Number With Axial Distance in a Rectangular Duct With 1/3 Aspect Ratio

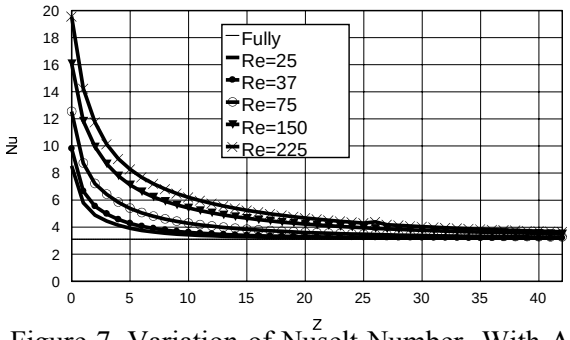

Figure 7. Variation of Nuselt Number With Axial Distance in a Rectangular Duct With 2/3 Aspect Ratio

Curves given for several values of Reynolds number and the same value of aspect ratio approach to the same limit, that is, the fully developed flow Nusselt number. At sufficiently higher values of Z and lower values of Reynolds number, the difference between the fully developed flow Nusselt number and local Nusselt becomes sufficiently small. For $1/3$, $2/3$ and $1/1$ aspect ratio, the fully developed flow Nusselt numbers are 3.96, 3.118 and 2.976 respectively. At $Z = 40$ and $\mathrm{Re} = 250$, Local Nusselt numbers are 4.068, 3.186 and 3.028, respectively, and decreasing yet. In the case of high values of Reynolds number, the difference between fully developed flow Nusselt number and local Nusselt number becomes greater than that of $\mathrm{Re} = 250$ at $Z = 40$.

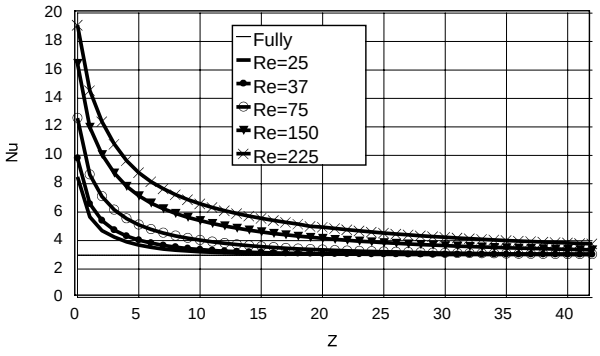

Figure 8. Variation of Nuselt Number With Axial Distance in a Square Duct

Figure 9, 10 and 11 illustrate the gradient of the wall pressure. Since the pressure is normalized by dynamic pressure, the lowest curve corresponds to the highest Reynolds number while the highest curve corresponds to the lowest Reynolds number. Figure 9, 10 and 11 indicate that the variation of pressure gradient almost vanishes before $Z = 10$.

As seen from Figure 6, 7 and 8, beyond $Z = 10$ the local Nusselt number displays a significant variation.

CONCLUSION

The hydrodynamic and thermal entrance region of rectangular ducts were analyzed for airflow. For the correction of pressure, a poison type differential equation was used. In solving pressure correction equation, Drichlet type boundary condition was used. Axial velocity profiles obtained from this analysis were different than that given by Schlichting (2) in shape. Distribution of Local Nusselt number and pressure gradient were calculated for three different aspect ratios and several values of Reynolds number at each aspect ratio, and results were graphically presented. Developing length of Nusselt number was longer than that of pressure gradient. The use of Newton-Raphson method provided a better convergence in solving finite difference equations.

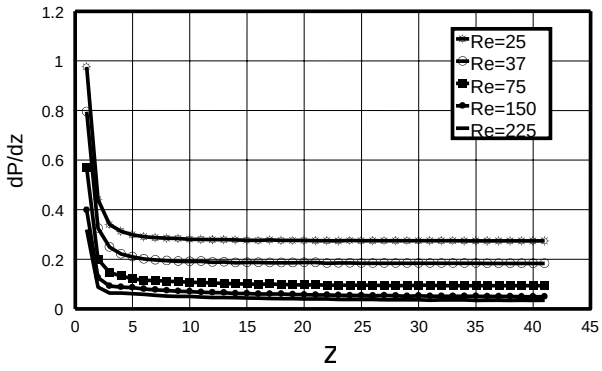

Figure 9. Axial Gradien of the Wall Pressure In a Rectangular Duct With 1/3 Aspect Ratio

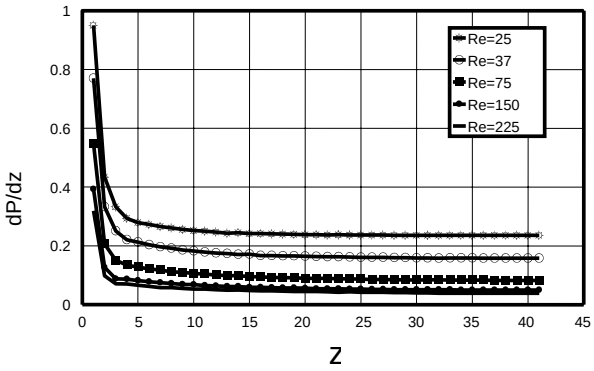

Figure 10.Axial Gradien of the Wall Pressure In a Rectangular Duct With 2/3 Aspect Ratio

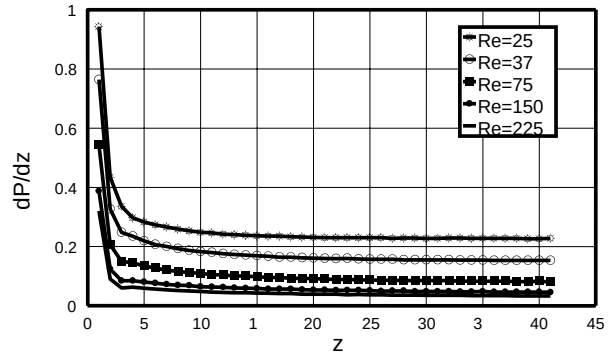

Figure 11. Axial Gradien of the Wall Pressure in a Square Duct.

NOMENCLATURE

A	area of the duct (m^2)
D_h	Hydraulic diameter (m)
Nu	Nusselt number
P	Pressure (Pa)
$\overline{P}$	$p \Big/ \frac{\rho w_\infty^2}{2}$
$\overline{P}_w$	Dimensionless pressure at the wall
P_r	Prandtl number
Re	Reynols number
T	Temperature (K)
T_{in}	Inlet temperature (K)
T_w	Temperature at the wall (K)
u	Velocity component in x coordinate (m/s)
v	Velocity component in y coordinate (m/s)
w	Velocity component in z coordinate (m/s)
U	u / W_∞
V	v / W_∞
W	w / W_∞
W_∞	Mean velocity (m/s)
x, y, z	Coordinate elements
X, Y, Z	$x / D_h , y / D_h , z / D_h$ respectively
X_m	Maximum value of X
Y_m	Maximum value of Y

Greek symbols

ρ	Density (kg/m^3)
θ	Dimensionless temperature
θ_m	Mean value of dimensionless temperature

REFERENCES

1. Nguyen ,V. T., and Maclaine-cross, I, I., Simultaneously Developing, Laminar Flow, Forced Convection in the Entrance Region of Parallel Plates, Journal of Heat Transfer, Vol. 113, p.113-842, November 1991.

2. Schlichting, H., Boundary Layer Theory, McGraw-Hill Publishing Company, New York, 1979

3. Cheng, C.H., Weng, C.J., Aung, W., Buoyancy-assisted Flow Reversal and Convective Heat Transfer in Entrance Region of a Vertical Duct, International Journal of Heat and Fluid Flow, Vol. 21, p. 403-411, 2000.

4. Gupta, R.C., On developing laminar non-Newtonian Flow in Pipes and Channels, Nonlinear Analysis, Vol.2, p. 171-193, 2001.

5. Magno, R. N. O., Macedo, E. N., Quaresma, J. N. N., Solution for the Internal Boundary Layer Equations in Simultaneously Developing Flow of Power-law Fluids within Parallel Plates Channels, Chemical Engineering Journal, Vol. 87, p.339-350, 2002.

6. Shyy, W., Advances in Heat Transfer, Vol. 24, p. 191-274, ISBN 0-12-020024-4, Academic Press, 1994.

7. Vradis, G., Zalak, V., Benston, J., Simultaneous Variable Solution of the Incompressible Steady Navier-Stock Equations in General Curvilinear Coordinate Systems., Journal of Fluid Engineering, Vol. 114, p.299-305, September 1992.

8. Spiga, M., and Morini, G.L., The developing Nuselt Number for Slug Flow in Rectangular Ducts, International Journal of Heat and Mass Transfer, Vol 41, p. 2799-2807, September 1998.

9. Sayed-Ahmed, M.E., Laminar heat transfer for thermally developing flow of a Herschel-Bulkley fluid in a Square Duct, Int. Com. Heat Mass Transfer, Vol.27, p.1013-1024, 2000.

10. Burden, R.L., and Douglas F. J., Numerical Analysis, PWS-KENT Publishing Company, Boston, 1989.

11. Kincaid, D., and Cheney, W., Numerical Analysis-Mathematics of Scientific Computing, Brooks/Cole Publishing Company, Pacific Grove, California, 1991.

12. Madhav, M.T., and Malin, M.R., The Numerical Simulation of Fully Developed Duct Flows, Appl. Math. Modeling, Vol. 21, p. 503-507, August 1997.